MedCrave
Step into the World of Research
Electrical & Electronic Technology Open Access Journal

Research Article

Open Access
CrossMark

On the analytical tuning of controllers for grid-coupled voltage source converter: frequency analysis

Abstract

This article presents frequency analysis of controllers parameters tuning methods for grid-coupled voltage source converter. In distributed power systems, the grid-coupled voltage source converter exists in pairs linked back-to-back through a DC-link capacitor. The grid-side converter is coupled to the grid through L, LC, or LCL filter. Each of the three analytical methods of pole-zero placement, Butterworth polynomial and Internal Model Control is analyzed and tested through simulation studies in a MATLAB Simulink environment for the three filter conditions. The results so obtained shows that even as any of the three methods can be adopted for efficient control performance, the IMC method presents the best option with the addition of minor loop in the DC-link voltage control loop. In this method, the usual problem of trial and error tuning of PI controller parameters is reduced to only selecting an appropriate bandwidth frequency for the closed loop control.

Keywords: back-to-back converter, filter, controllers parameters, grid-connection, filter current, dc-link voltage

Volume 1 Issue 1 - 2017

Cajethan M Nwosu, Cosmas U Ogbuka, Stephen E Oti
DDepartment of Electrical Engineering, University of Nigeria, Nigeria

Correspondence: Cajethan M Nwosu, Department of Electrical Engineering, University of Nigeria, Nigeria, Email cajethan.nwosu@unn.edu.ng

Received: July 22, 2017 | **Published:** November 08, 2017

Introduction

The grid conditions determine what the output voltage of a grid connected power converters should be. Control of the output voltage of these power converters is by this condition not possible. The power converters are however, not directly connected to the grid. The conventional method to interface these converters to the grid is through filters.[1,2] The duty of the filter is to reduce the current harmonics around the switching frequency of the converter. The current harmonics is capable of polluting the grid with the effect of disturbing any connected equipment.[2,3] In some practical applications, the converter is not just a single three-phase converter but two back-to-back converters usually interfacing two AC systems. The two converters are linked to each other through a DC-link. The converter adjacent to the grid is in this work referred to as grid-side converter (GSC). The scope of this paper is limited to the analysis of control of the filter current and the influence of the filter on the grid and the grid-side converter with the DC-link. The filter can be a simple L, LC or LCL filter. The choice of any scheme may depend on cost, size, or dynamic performance. The filter current injected into the grid becomes the control variable since the grid voltage can't be controlled. The filter input current is usually sensed and given back as feedback to close the control loop. Hence, the transfer function which decides the closed loop performance of the filter is the transfer function between output current and input voltage of the filter for zero grid voltage.[1] Usually the current control is implemented in a dq-rotating frame in order to obtain a control with rapid dynamic response. The dq components of converter output currents are controlled using state-of-art synchronous frame PI control.[4] Generally the current control is designed on per phase basis and the decoupling terms are added to allow such design. This decreases the order of system and hence simplifies controller design.[5]

In the past decades, PI controller has found wide applications in industrial process controls. This is majorly due to simplicity of its control law and the few tuning parameters. However, research is still on going on methods of obtaining the appropriate parameters. The researched tuning processes include but not limited to trial and error methods, feature based methods, analytical methods, optimization based methods, loop shaping methods, and auto-tuning methods.[6] Among others, the analytical methods are the preferred parameter tuning process in the control of grid-connected power converters. In this paper, three kinds of analytical methods: pole-zero placement method, Butterworth polynomial method and Internal Model Control (IMC) method are each adopted for the tuning of controllers parameters for L, LC, and LCL filter interfaced grid-connected power converters. In effect pole-zero placement method and Butterworth polynomial method are similar in the sense that the primary objective of both methods is to place the closed-loop poles at the desired location in the left-half of the frequency domain. These methods, their controllers' parameters results and the effects of the application of the parameters on the dynamic responses of the system are compared. The filter interface constitutes the PI controller process plant for the control of filter current injected into the grid.

System modeling

Models for the L, LC, and LCL filters shall be developed with a view to generating the respective transfer function for the grid current control. The transfer function which decides the closed loop performance of the filter is the transfer function between output current and input voltage of the filter for zero grid voltage.[1] (Figure 1) shows a one-line diagram of the converter connected to the grid through per-phase filter inductance. v_{DC} is the DC-link voltage; v_c and i_c are converter voltage and current respectively while v_g and i_g are grid voltage and current respectively.

L Filter

The voltage balance across the three inductors can be written as:

$$\begin{bmatrix} v_a \\ v_b \\ v_c \end{bmatrix} = R\begin{bmatrix} i_a \\ i_b \\ i_c \end{bmatrix} + \dot{p}\begin{bmatrix} i_a \\ i_b \\ i_c \end{bmatrix} + \begin{bmatrix} v_{a1} \\ v_{b1} \\ v_{c1} \end{bmatrix} \quad (1)$$

where v_a, v_b, and v_c are the three phase grid voltages, v_{a1}, v_{b1}, and v_{c1} are the front-end converter voltages, and i_a, i_b, and i_c are the line currents. L and R are the filter inductance and resistance, and $p = \frac{d}{dt}$. Applying phase and rotation transformations to Eq. (1) results in:

$$v_d = R_d + Lpi_d - \omega_e L_q + v_{d1} \quad (2)$$

$$v_q = R_q + Lpi_q + \omega_e L_d + v_{q1} \quad (3)$$

v_d and v_q, i_d and i_q, and v_{d1} and v_{q1} are the d- and q-axis components of the grid voltages, line currents, and front-end converter voltages respectively. The terms $\omega_e Li_d$ and $\omega_e Li_q$ cause a cross-coupling of the d- and q-axis, while the last terms are the d- and q-axis converter terminal voltages. The system is said to be coupled because the inductance matrix is not diagonal. This means that any changes in voltage component in d- or q-axis results in changes in both current components. The third and the last terms are treated as disturbances on the output. The PI controller tracks the i_d and i_q errors to give v_d and v_q respectively. To ensure good tracking of these currents, the cross-related flux terms are added to v_d and v_q to obtain the reference voltages. The dynamics of the d-q reference frame are:

$$Lpi_d = v_d - R_d + \omega_e L_q + v_{d1} \quad (4)$$

$$Lpi_q = v_q - R_q - \omega_e L_d + v_{q1} \quad (5)$$

The transfer function from $\mathbf{v}_{dq}$ as input to $\mathbf{i}_{dq}$ as output yields:

$$G(p) = \frac{i_d(p)}{v_d(p)} = \frac{i_q(p)}{v_q(p)} = \frac{1}{Lp + R} \quad (6)$$

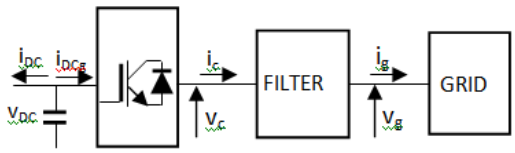

Figure 1 Per-phase simple filter as an interface between power converter and grid

LC Filter

The filter capacitor in an LC filter provides a low-impedance path for the high frequency PWM ripple current and, thus, attenuates the content of current ripple in the utility current.[7] For a balanced three-phase system, the d-q dynamic equations for the grid current control are same as Eqns. (4) and (5). On the assumption that the parasitic grid impedances are neglected, the transfer function of grid current to inverter voltage is same for L and LC filters. Therefore, the size of inductor does not change from L to LC filter.

LCL Filter

In order to obtain the transfer function of the LCL filter, the one phase electrical diagram in (Figure 2) is considered. The subscripts 'c' and 'g' denote converter-side and grid-side components respectively. The components of the filter on each phase are considered to be identical, so the circuit below is suitable for the other two phases. Using Kirchoff's laws, the filter model in s-plane can be written with the following equations:[8]

$$i_c - i_{cf} - i_g = 0 \quad (7)$$

$$v_c - v_{cf} = i_c(Lp + R_c) \quad (8)$$

$$v_{cf} - v_g = i_g(Lp + R_g) \quad (9)$$

$$v_{cf} = i_{cf}\left(\frac{1}{Cp}\right) \quad (10)$$

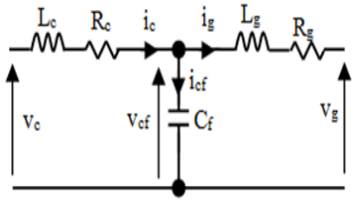

Figure 2 One phase electrical circuit of an LCL filter.

In the mathematical analysis of the transfer function, the grid voltage is assumed to be an ideal voltage source and it represents a short circuit for harmonic frequencies, it is therefore set to zero: $v_g = 0$.

From equations (9) and (10), the following relation can be written:

$$i_g(Lp + R_g) = i_{cf}\left(\frac{1}{Cp}\right) \quad (11)$$

from which we obtain:

$$i_{cf} = i_g(p^2 C_f L_g + Cp R_g) \quad (12)$$

Equation (8) can be re-written as:

$$v_c = v_{cf} + i_c(Lp + R_c) \quad (13)$$

By introducing (9), (7) and then (12) into (13), the converter voltage can be written as:

$$\begin{aligned} v_c &= i_g(Lp + R_g) + (i_g + i_{cf})(Lp + R_c) \\ &= i_g(Lp + R_g) + (i_g + i_g\{p^2 C_f L_g + Cp R_g\})(Lp + R_c) \end{aligned} \quad (14)$$

$$\Rightarrow$$

$$v_c = i_g(Lp + R_g + Lp + R_c + (p^2 C_f L_g + Cp R_g)(Lp + R_c) \quad (15)$$

The transfer function of the filter can be obtained as:

Citation: Nwosu CM, Ogbuka CU, Oti SE. On the analytical tuning of controllers for grid-coupled voltage source converter: frequency analysis. *Electric Electron Tech Open Acc J.* 2017;1(1):33–41. DOI: 10.15406/eetoaj.2017.01.00007

$$H(p)=\frac{i_g}{v_c}=\frac{1}{p^3L_gL_cC_f+p^2(L_gR_cC_f+L_cR_g)+p(L_g+L_c+R_gR_cC_f)+R_g+R_c} \quad (16)$$

The transfer function of equation (16) is particularly useful for stability and harmonic analysis of LCL filter. For the design of the controller, the filter capacitor is neglected to obtain the d-q reference frame dynamic equations similar to (4) and (5) as:

$$L_T\dot{p}_q = v_q - R_T i_q - \omega_e L_T i_d + v_{q1} \quad (17)$$

$$L_T\dot{p}_q = v_q - R_T i_q - \omega_e L_T i_d + v_{q1} \quad (18)$$

where $L_T = L_c + L_g$, and $R_T = R_c + R_g$.

The system plant is obtained as:

$$G(p)=\frac{i_d(p)}{v_d(p)}=\frac{i_q(p)}{v_q(p)}=\frac{1}{pL_T+R_T} \quad (19)$$

Controller's design

The control of the grid-side converter consists of a fast inner current control loop, which controls the current through the line inductance, and an outer slower control loops that regulate the DC-link voltage and the reactive power exchanged between the GSC and the grid. The structure of the d-q current-control, DC-link voltage control and the reactive power exchange control loops is shown in Figure 3. For unity power factor, the reactive power reference current i_q^* is set to zero.

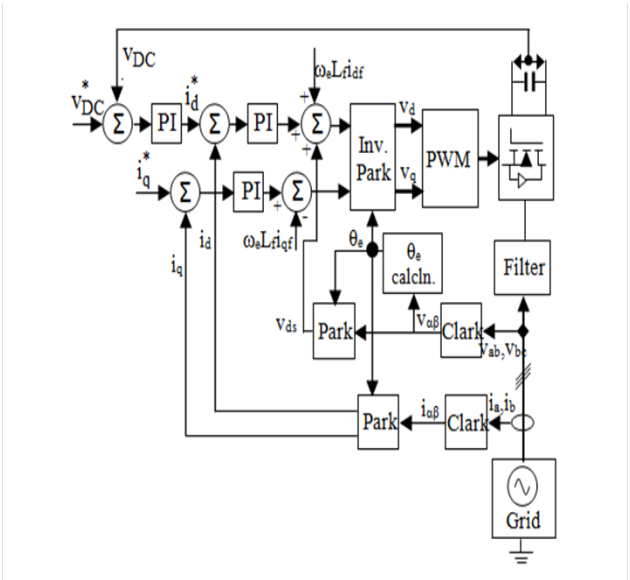

Figure 3 Current-control loop of grid-side converter.

Current controller

The term $\omega_e Li_{dq}$ in Figure 3 is the d-q rotational emfs which appear as cross-coupling terms due to the transformation. The transfer function of the PI controller is given by:

$$C(p)=\left(k_{pdq}+\frac{k_{idq}}{p}\right)=k_{pdq}\left(1+\frac{1}{pT_i}\right) \quad (20)$$

where k_{pdq} is the d and q components proportional gain, k_{idq} is the integral gain of the d and q components controllers, and T_i is the integration time obtained as the ratio of the proportional gain to the integral gain. The representations of d-q in the gains mean that the d and q axis currents are controlled via independent regulators.

The PI current controller in each axis generates the control signals v_d^{ref} and v_q^{ref} in a way to regulate the currents i_d and i_q, respectively. These signals are then synthesized by the converter and, so, injected in the electrical grid. In,[9] it is assumed that there are no delays and so the converter transfer function G_{conv} also known as converter constant k_c may be considered ideal because $v_d^{ref}=v_d$ and $v_q^{ref}=v_q$. In this paper however, the influence of k_c is taken into consideration in all the three methods under analysis. For the grid-side converter, k_c may be modeled as:[10]

$$k_c=\frac{m_1 v_{DC}}{2V_{tri}} \quad (21)$$

where m_1 is the grid-side converter modulation depth, v_{DC} is the DC-link voltage, and V_{tri} is the amplitude of the triangular carrier which is usually compared with the reference signal to generate the converter switching pulses. Tuning of PI controllers entails obtaining the appropriate parameters, proportional gain and the integration time in order to obtain a control with rapid dynamic response. This paper focuses on generating the PI controllers' parameters through the three analytical methods.

DC-link voltage controller

The dynamics of the DC-link may be rewritten as:

$$C\frac{dv_{DC}}{dt}=\frac{3}{2\sqrt{2}}m_1 i_d - i_{DC} \quad (22)$$

Applying Laplace Transform to (22) yields:

$$pCv_{DC}(p)=\frac{3}{2\sqrt{2}}m_1 i_d(p)-i_{DC}(p) \quad (23)$$

The transfer function from i_d as input to v_{DC} as output yields:

$$\frac{v_{DC}(p)}{i_d(p)}=G_v(p)=k_v\frac{1}{pC} \quad (24)$$

where $k_v=\frac{3}{2\sqrt{2}}m_1$. The component i_{DCg} represent the grid-side DC-link current. The other component i_{DC}, may bear any designation based on the second AC system which the filter interfaces with the grid. The i_{DC} component is regarded as a disturbance in the control and may be neglected.

Citation: Nwosu CM, Ogbuka CU, Oti SE. On the analytical tuning of controllers for grid-coupled voltage source converter: frequency analysis. *Electric Electron Tech Open Acc J.* 2017;1(1):33–41. DOI: 10.15406/eetoaj.2017.01.00007

Pole-zero placement method

The objective of pole-zero placement technique is to place the closed loop poles at desired locations. Here, complete knowledge of the transfer function is needed to calculate the appropriate controller parameters. Desired closed loop poles are specified, and the controller parameters that move the poles to these positions are analytically calculated. The filter plant in each case is of first order so that a direct pole placement technique is used all through. The parameters of the controller are calculated, such that the closed-loop poles which are a pair of complex conjugates are located at desired pole locations, specified by their undamped natural frequency ω_0 and damping ratio ξ as:

$$p_1 = -\xi\omega_0 + j\omega_0\sqrt{1-\xi^2} = -\sigma + j\omega \tag{25}$$

$$p_2 = -\xi\omega_0 - j\omega_0\sqrt{1-\xi^2} = -\sigma - j\omega \tag{26}$$

The complex conjugate poles lie in the left-half s-plane as shown in Figure 4.

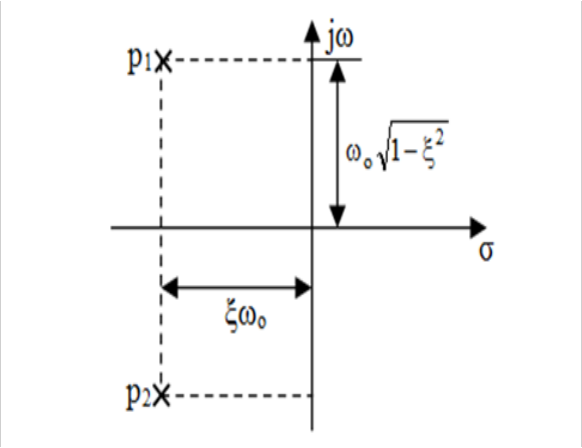

Figure 4 Complex conjugate poles

Current controller

In order to apply the three analytical methods in the determination of the current controller parameters, a design example is taken into consideration. The LCL filter-based active rectifier has the following components: L_c=L=17.7mH, L_g=5.7mH, and C_f=3.45μF with a resonance frequency around 1.30kHz. In addition, R_c=R_g=0.1Ω is assumed in this paper. The filter has been designed to reduce the switching current ripple to less than 1% of the rated current. The system parameters considered for calculating the components for the filter are shown in (Table 1).[11]

The d and q control loops have the same dynamics, so the same tuning of the PI parameters is adopted for the two current control axes. The voltage feed forward and the decoupling between the d and q axes in the current control loop of Figure 3 are neglected in the analysis for the generation of the controller parameters as they are considered as disturbances. Employing a more general PI controller transfer function as:

$$C_c(p) = \frac{k_P\, p + k_I}{p} \tag{27}$$

and the plant model in (19), the open loop $G_{oc}(p)$ and closed loop $G_{clc}(p)$ transfer functions are as follows:

$$G_{oc}(p) = \frac{k_c k_P\, p + k_c k_I}{p(L_T p + R_T)} \tag{28}$$

$$G_{clc}(p) = \frac{\frac{1}{L_T}(k_c k_P\, p + k_c k_I)}{p^2 + \frac{(R_T + k_c k_P)}{L_T} p + \frac{k_c k_I}{L_T}} \tag{29}$$

Calculation of the closed-loop poles involves solving characteristic equation of the control system:

$$p^2 + \frac{(R_T + k_c k_P)p}{L_T} + \frac{k_c k_I}{L_T} = 0 \tag{30}$$

Table 1 Parameters for calculating the filter components

Grid Voltage (V)	230
Output Power of the Converter (kVA)	1.5
DC-link Voltage (V)	550
DC-link capacitor (mF)	2.4
Grid Frequency (Hz)	50

Knowing that a 2nd order system is characterized by the characteristic equation:

$$p^2 + 2\xi\omega_o p + \omega_o^2 = 0 \tag{31}$$

where ξ and ω_o correspond to the damping ratio and the natural frequency of the system oscillation, respectively. The gains k_{pc} and k_{ic} can be obtained by equating (30) and (31), so that:

$$\omega_o^2 = \frac{k_c k_I}{L_T} \Rightarrow k_I = L_T \omega_o^2 / k_c \tag{32}$$

and

$$2\xi\omega_o = \frac{R_T + k_c k_P}{L_T}$$
$$\Rightarrow k_P = (2\xi\omega_o L_T - R_T)/k_c \tag{33}$$

The grid-side converter constant is obtained by assuming a unit value for the V_{tri}, 0.75 for m_1, and substituting the DC-link voltage value in Table 1. The natural frequency of the system oscillation and the damping ratio may be established by selecting the settling time t_s and maximum overshoot M_p. In this paper, $t_s \leq 5$ms and $M_p \leq 4.6\%$ are selected. $M_p = e^{-\frac{\xi}{\sqrt{1-\xi^2}}} = 0.046$ corresponds to ξ=0.7. From $t_s = \frac{4}{\xi\omega_o} = 0.005s$, ω_o is obtained as 1142.86 rad/s. Substituting ω_o into (32) and ω_o and ξ into (33), the controller parameters are obtained.

DC-link voltage controller

The PI controller transfer function for the DC-link voltage control is given as:

Citation: Nwosu CM, Ogbuka CU, Oti SE. On the analytical tuning of controllers for grid-coupled voltage source converter: frequency analysis. *Electric Electron Tech Open Acc J.* 2017;1(1):33–41. DOI: 10.15406/eetoaj.2017.01.00007

$$C_v(p) = \frac{k_P p + k_I}{p} \quad (34)$$

The open loop $G_{ov}(p)$ and closed loop $G_{clv}(p)$ transfer functions are as follows:

$$G_{ov}(p) = \frac{k_v k_P p + k_v k_I}{p(p^2 + \frac{1}{C})} \quad (35)$$

$$G_{clv}(p) = \frac{\frac{1}{C}(k_v k_P p + k_v k_I)}{p^2 + \frac{k_v k_P}{C} p + \frac{k_v k_I}{C}} \quad (36)$$

Comparing the denominator of (36) with (31) yields:

$$k_I = \omega_o^2 C / k_v \quad (37)$$

$$k_P = 2\xi\omega_o C / k_v \quad (38)$$

Substituting ω_o and ω_o and ξ obtained previously into (37) and into (38) respectively, the controller parameters are obtained.

Butterworth polynomial method

The Butterworth polynomial method of controller parameter tuning like the pole-zero placement method aims at optimizing the closed-loop eigenvalue locations. In this case the eigenvalues are located uniformly in the left-half s-plane on a circle with bandwidth frequency of the controller denoted in this paper by α_o as radius, with its center at the origin,[13] as shown in Figure 5. The PI parameters are determined through comparing the coefficients of the Butterworth polynomial with the denominators of the corresponding transfer functions as in pole-zero placement method. The Butterworth polynomial for a transfer function with a second order denominator is given as:

$$p^2 + \sqrt{2}p\alpha_o + \alpha_o^2 = 0 \quad (39)$$

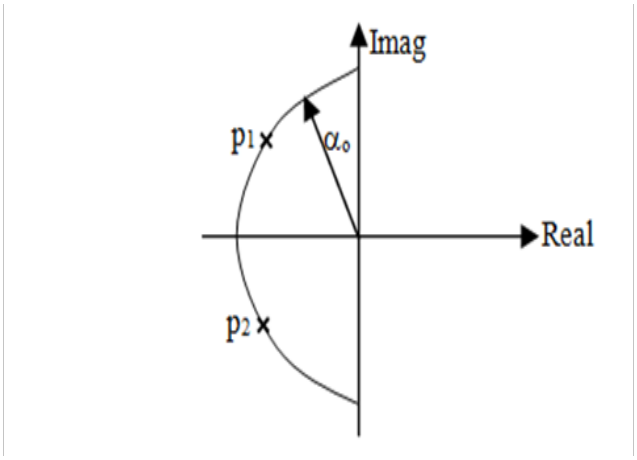

Figure 5 Poles location for 2nd order Butterworth polynomial.

Unlike in the pole-zero placement method, where the settling time t_s, and the maximum overshoot M_p must first be specified in order to calculate the natural frequency of the system oscillation and the damping ratio prior to obtaining the controller parameters, the Butterworth polynomial method and the IMC method are both concerned with selection of only the bandwidth frequency of the control loop. The method of selecting the bandwidth frequency is explained in the next section.

Current controller

To design the inner-loop current controllers, the relation between the d-q components of voltages and currents is first established from (17) and (18) as:

$$v_d = R_T i_d + L_T \dot{p}_d - \omega_e L_T i_q + k_c m_{1d} v_D \quad (40)$$

$$v_q = R_T i_q + L_T \dot{p}_q + \omega_e L_T i_d + m_{q1} v_D \quad (41)$$

Equations (40) and (41) are coupled and nonlinear. In order to apply the linear PI controller, the nonlinear equations are linearized by moving the nonlinear parts of the two equations to one side to have:

$$R_T i_d + L_T \dot{p}_d = v_d + \omega_e L_T i_q - k_c m_{1d} v_D \quad (42)$$

$$R_T i_q + L_T \dot{p}_q = v_q - \omega_e L_T i_d - m_{q1} v_D \quad (43)$$

From (42) and (43), the current control loop equations are obtained as:

$$R_T i_d + L_T \dot{p}_d = (R_T + p L_T) i_d = k_C (i_d^* - i_d) \quad (44)$$

$$R_T i_q + L_T \dot{p}_q = (R_T + p L_T) i_q = k_C (i_q^* - i_q) \quad (45)$$

where $k_C = \left(k_P + \frac{k_C}{p}\right)$ is the current controller. Again, the d and q control loops have the same dynamics, so the same tuning of the PI parameters is adopted for the two current control axes. Thus (44) and (45) may be expanded in one to have:

$$(R_T + p L_T) i_q = \left(k_P + \frac{k_C}{p}\right) i_q^* - \left(k_P + \frac{K_C}{p}\right) i_q \quad (46)$$

from which we obtain:

$$\frac{i_d}{i_d^*} = \frac{i_q}{i_q^*} = \frac{\frac{1}{L_T}(p + k_C)}{p^2 + p\frac{1}{L_T}(R_T + k_P) + \frac{1}{L_T} k_C} \quad (47)$$

Comparing the denominator of (47) with the Butterworth second order polynomial of (39) yields:

$$k_P = \sqrt{2}\alpha_o L_T - R_T \quad (48)$$

$$k_C = L_T \alpha_o^2 \quad (49)$$

where α_o is the bandwidth frequency of the current controller.

DC-link voltage controller

The DC-link voltage dynamics may be given by:

$$Cpv_D = \frac{3}{2}(m_d i_d + m_q i_q) + \frac{3}{2}(m_d i_d + m_q i_q) \quad (50)$$

Citation: Nwosu CM, Ogbuka CU, Oti SE. On the analytical tuning of controllers for grid-coupled voltage source converter: frequency analysis. *Electric Electron Tech Open Acc J.* 2017;1(1):33–41. DOI: 10.15406/eetoaj.2017.01.00007

where m_{dg} and m_{qg} are the d and q-axis modulation indexes of the GSC and m_d and m_q are the d and q-axis modulation indexes of the second converter not shown, respectively. In order to generate the d-component of the reference current i_{gd}^* for the inner loop, (50) may be re-written as [13]:

$$Cpv_{DC} = \frac{3}{2}\left(m_{gd} i_{gd} + m_{gq} i_{gq}\right) + \frac{3}{2}\left(m_d i_d + m_q i_q\right) = \delta_V \tag{51}$$

Equation (50) may also be re-written as:

$$Cpv_{DC} = \delta_V = k_V\left(v_{DC}^* - v_{DC}\right) \tag{52}$$

where k_V is the PI controller for DC-voltage control given as:

$$k_V = k_{PV} + \frac{k_{IV}}{p} \tag{53}$$

In an expanded form, (52) will be:

$$Cpv_{DC} = \left(k_{PV} + \frac{k_{IV}}{p}\right)v_{DC}^* - \left(k_{PV} + \frac{k_{IV}}{p}\right)v_{DC} \tag{54}$$

from which:

$$\frac{v_{DC}}{v_{DC}^*} = \frac{\frac{1}{C}\left(k_{PV} p + k_{IV}\right)}{p^2 + p\frac{k_{PV}}{C} + \frac{k_{IV}}{C}} \tag{55}$$

Comparing the denominator of (55) with Butterworth second order polynomial, the PI controller gains are obtained as:

$$k_{PV} = \sqrt{2}\alpha_o C \tag{56}$$

$$k_{IV} = \alpha_o^2 C \tag{57}$$

where α_o is the bandwidth frequency of the DC-link voltage controller.

Internal model control method

The internal model control (IMC) structure has been a very popular one in process control application, especially as applied to AC machine current and speed controls.[14–16] The prime benefit of this structure is the deployment of the model of the plant and the desired closed-loop bandwidth in the determination of the controller parameters (gain and integration time). In this case, the tuning problem, which for a PI controller involves adjustment of two parameters, is reduced to the selection of one parameter only, the desired closed-loop bandwidth α. The idea behind IMC is to augment the error between the process, *G(p)* and a process model, $\hat{G}(p)$ by a transfer function *C(p)*; see (Figure 6).

Current controller

The IMC structure uses an internal model $\hat{G}(p)$ in parallel with the controlled system plant *G(p)*. For an AC machine, u and y could be the stator voltage and current vectors, respectively, while $x = [i_d^{ref}, i_q^{ref}]^T$ is the current set point (reference) vector. The control loop is augmented by a block *C(p)*, the so called IMC controller. $G(p)$, $\hat{G}(p)$ *and* $C(p)$ are all transfer function matrices. It should be noted that, if the internal model is perfect, i.e. $\hat{G}(p) = G(p)$ there is no internal feedback loop in Figure 6 and the closed-loop system has the transfer function matrix:

$$G_c(p) = G(p)C(p) \tag{58}$$

Controller design is a matter of choosing the "right" transfer function C(s). One common way is:[17]

$$C(p) = \left(\frac{\alpha}{p+\alpha}\right)^n G^{-1}(p) \tag{58}$$

where n is chosen so that C(p) become proper, i.e., the order of the denominator is equal to or greater than that of the numerator. The parameter α is a design parameter, which for n=1, is set to the desired bandwidth of the closed-loop system. For a first-order system, n=1 is sufficient. For the inner-current control, the controller then typically becomes an ordinary PI controller:

$$C_C(p) = \frac{\alpha}{p} G_C^{-1}(p) = k_{PC} + \frac{k_{IC}}{p} \tag{59}$$

With $G_C(p)$ comprising the product of the grid-side converter constant and the system plant as:

$$G_C(p) = \frac{k_c}{L_T p + R_T} \tag{60}$$

the PI controller gains are:

$$k_{PC} = \frac{\alpha L_T}{k_c};\ k_{IC} = \frac{\alpha R_T}{k_c} \tag{61}$$

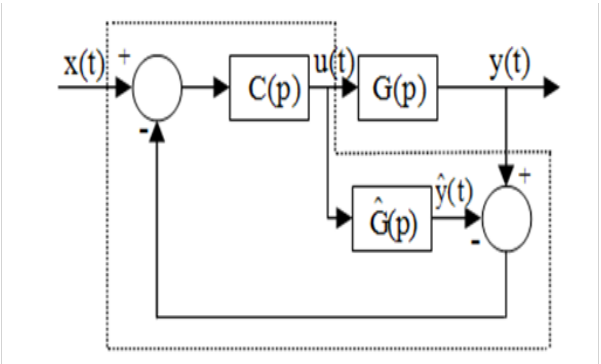

Figure 6 Principle of IMC.

DC-link voltage controller

For the DC-link voltage control, the PI controller is:

$$C_V(p) = \frac{\alpha}{p} G_V^{-1}(p) = k_{PV} + \frac{k_{IV}}{p} \tag{62}$$

With $G_V(p)$ comprising the product of the DC-link voltage control constant and the system plant as:

$$G_V(p) = \frac{k_V}{pC} \tag{63}$$

Citation: Nwosu CM, Ogbuka CU, Oti SE. On the analytical tuning of controllers for grid-coupled voltage source converter: frequency analysis. *Electric Electron Tech Open Acc J.* 2017;1(1):33–41. DOI: 10.15406/eetoaj.2017.01.00007

from which the controller gains are obtained as:

$$k_{pV} = \frac{\alpha C}{k_V};\ k_{iV} = 0 \tag{64}$$

The closed-loop bandwidth frequency α is selected in relation to the converter switching frequency. In order to mitigate the degrading of the system performance, it is recommended that the angular switching frequency ω_{sw} should at least be five times the closed-loop bandwidth:[18]

$$\omega_{sw} \geq 5\alpha \tag{65}$$

A chosen converter angular switching frequency of 12252 rad/s (or1950Hz) corresponds to a bandwidth of 2450 rad/s. The current control closed-loop bandwidth is thus selected to be 2000 rad/s while the DC-link voltage control bandwidth is 200 rad/s.

Simulation studies

The controllers' parameters for the current control and DC-link control for the three methods under study are generated for L, LC, and LCL filters. These parameters which are used in the simulation studies are shown in Table 2. Figure 7 is the root-locus map showing the pole-zero locations for the closed loop current control. The dominant poles have a damping of 0.7 at a frequency of 1140 rad/s. The percentage maximum overshoot of 4.6 corresponds with the calculated value. The root-locus map for the closed loop current control resulting from the Butterworth polynomial method of tuning controller parameters is shown in (Figure 8-10) show the Bode plots and step response plots for the three controller parameters tuning methods for the inner current control. (Figures 11 &12) show the Bode plots and step response plots for the three controller parameters tuning methods for the DC-link voltage control.

Table 2 Gain parameters for the three analytical methods

Method	L or LC filter	LCL filter
Pole-placement	K_{PC}=0.137	K_{PC}=0.181
	K_{IC}=112.090	K_{IC}=148.186
	K_{PV}=4.827	K_{PV}=4.827
	K_{IV}=3.941	K_{IV}=3.941
Butterworth polynomial	K_{PC}=49.963	K_{PC}=65.985
	K_{IC}=70800	K_{IC}=93600
	K_{PV}=0.679	K_{PV}=0.679
	K_{IV}=96.000	K_{IV}=96.000
IMC method	K_{PC}=0.172	K_{PC}=0.227
	K_{IC}=0.970	K_{IC}=0.970
	K_{PV}=0.603	K_{PV}=0.603
	K_{IV}=0.000	K_{IV}=0.000

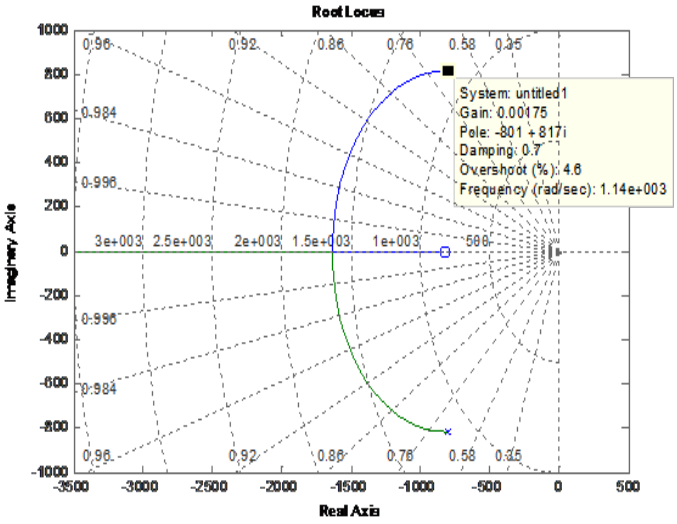

Figure 7 Root-locus map of the closed loop current control using pole-placement method.

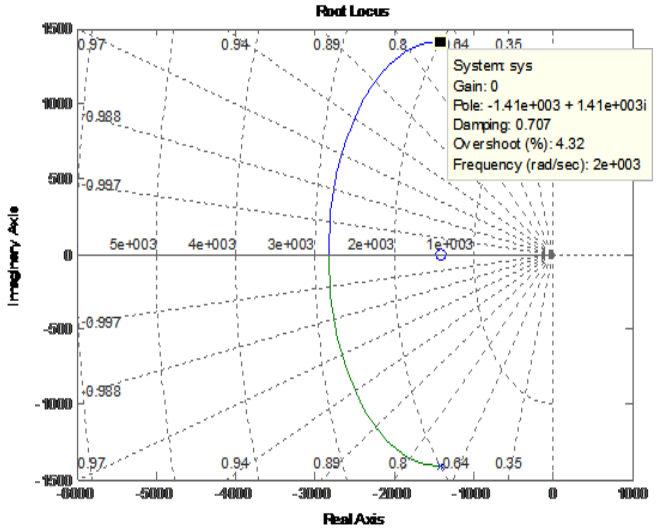

Figure 8 Root-locus map of the closed loop current control using Butterworth polynomial method.

Discussion of results

Each of the three analytical tuning techniques for the controllers' proportional gains, integral gains, and integration times can effectively be adopted to maintain stable system operation. The root-locus map of (Figure 7) confirms the assumed data for overshoot and damping ratio and calculated natural frequency of operation of the system for the pole-placement method. For same value of closed loop control bandwidth frequency chosen for the Butterworth polynomial and IMC methods, the Butterworth polynomial root-locus map of (Figure 8) share similar characteristics with that of (Figure 7). These similarities can easily be observed in Bode plots of Figure 9 and step response plots of (Figure 10). Considering the current control and the DC-link voltage control, it is observed however, that while the IMC method gives better performance for the current control, the pole-placement method gives better performance for the DC-link voltage control. The settling times (a measure of the dynamic response of system to transients) for the current control are $3x10^{-3}$s, $4.6x10^{-3}$s, and $8x10^{-}$

^{3}s for IMC, Butterworth polynomial, and pole-placement methods respectively. In the same order, their phase margins (a measure of the stability of feedback systems) are 180°, 127°, and 126°. Unlike the other two methods, the IMC method simulates a critical damping criterion as evidenced in Figure 10 with closed loop control negative real poles. For the DC-link voltage control, the pole-placement and IMC methods share some similarities. However, while the phase margin for the pole-placement method is 178°, the phase margin for IMC method is -180°. The negative phase margin is an indication that the use of IMC method for the DC-link voltage controller parameters results in instability of the controller system. This instability emanated from the existence of pole at the origin of the DC-link system plant. One solution for the instability is to add an inner feedback loop for active damping in the voltage control loop. The critical damping criterion of the IMC method exhibited in the current control is also extended in the DC-link voltage control. Of the three analytical tuning methods, the Butterworth polynomial method exhibits consistency in the phase margin, overshoot, and damping ratio for the current control and DC-link voltage control.

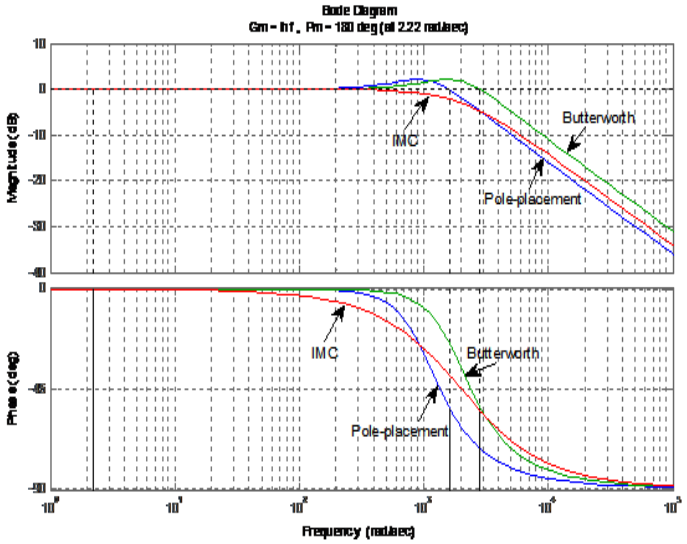

Figure 9 Bode plots for the three controllers' parameters tuning methods for the inner current control.

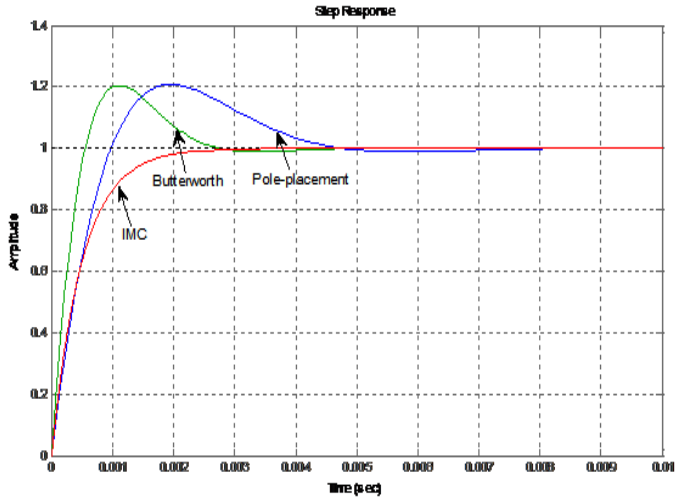

Figure 10 Step response plots for the three controllers' parameters tuning methods for the inner current control.

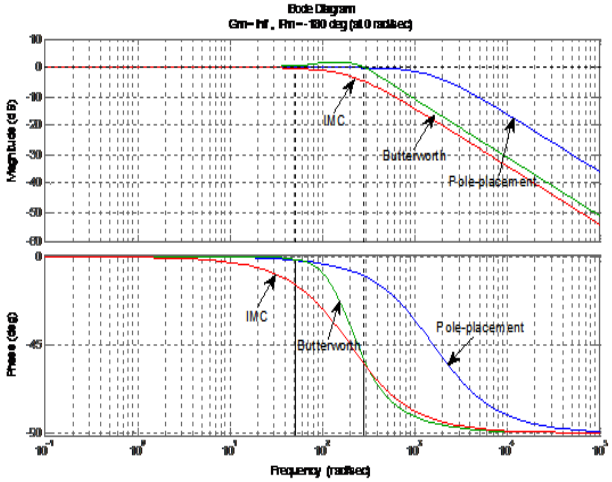

Figure 11 Bode plots for the three controllers' parameters tuning methods for DC-link voltage control.

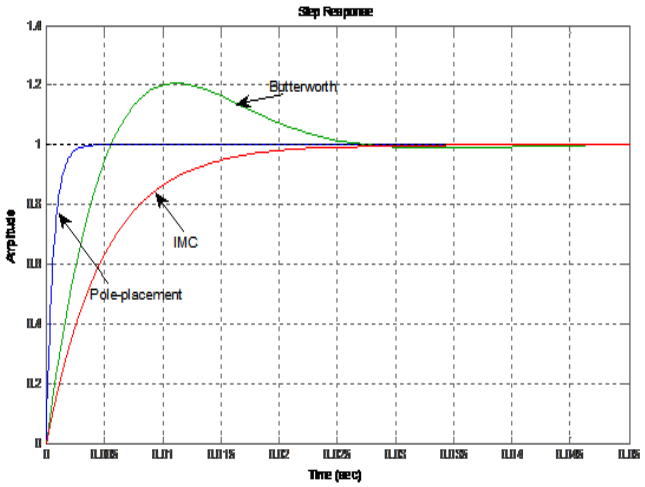

Figure 12 Step response plots for the three controllers' parameters tuning methods for DC-link voltage control.

Conclusion

Detailed study of analytical tuning of controllers for grid-coupled voltage source converter has been carried out. It is concluded that any of the three methods under study can effectively be adopted for good performance operation for the control system. However, with the addition of minor loop in the DC-link voltage control loop, the IMC method presents the best option owing to its capability to simulate a critical damping criterion both for current control and voltage control. Here, the problem of controller parameter tuning is reduced to only the selection of appropriate bandwidth frequency of the closed loop control. The additional inner loop in the DC-link voltage control has been established to have the capacity to damp the DC-link current component disturbance i_{DC}, with the same bandwidth as the DC-link voltage control loop. Due to the consistency in the phase margin, overshoot, and damping ratio for the current control and DC-link voltage control exhibited in the Butterworth polynomial analytical method, it becomes the second choice after the IMC method. Like the IMC approach, it only requires proper selection of bandwidth frequency of the closed loop control as against the initial specification of settling time and percentage overshoot prior to obtaining the damping ratio and natural frequency of system oscillation.

Citation: Nwosu CM, Ogbuka CU, Oti SE. On the analytical tuning of controllers for grid-coupled voltage source converter: frequency analysis. *Electric Electron Tech Open Acc J.* 2017;1(1):33–41. DOI: 10.15406/eetoaj.2017.01.00007

Acknowledgments

None.

Conflict of interest

The author declares no conflict of interest.

References

1. BC Parikshith, Vinod J. Higher Order Output Filter Design for Grid Connected Power Converters in Proceeding of Fifteenth National Power Systems Conference (NPSC), IIT Bombay, India; 2008. p. 614–619.
2. Liserre M, Dell Aquila A, Frede Blaabjerg. Stability Improvements of an LCL–filter Based Three–phase Active Rectifier in Proceeding of IEEE Power Electronics Specialists Conference; 2002. p. 1195 – 1201.
3. Liserre M, Blaabjerg F, Hansen S. Design and Control of an LCL–Filter–Based Three–Phase Active Rectifier. *IEEE Trans Ind Appl*. 2005;41(5):1281–1291.
4. Krishnan R, Blabjerg F. Control in Power Electronics, selected problems. USA: Academic Press; 2002.
5. Shahil. State Feedback Control & Sensorless Operation of Inverters. 2012.
6. Van der Zalm GM. Tuning of PID–Type Controllers: Literature Overview DAF–report nr. 51051104–050, Technical University Eindhoven, Netherlands; 2004.
7. Blasko V, Kaura V, (1997) A Novel Control to Actively Damp Resonance in Input LC Filter of a Three–Phase Voltage Source Converter. *IEEE Trans Ind Appl*. 1997;33(2):542–550.
8. Julean A. Active Damping of LCL Filter Resonance in Grid Connected Applications, Master Thesis, Aalborg University, Denmark.
9. Lopes C, Vieira JPA, Nunes MVA, et al. Using Genetic Algorithm to Tune PI–Controllers for the Direct–Drive Synchronous Wind Generators. 2012:1–30.
10. Pena R, Clare JC, Asher GM. Doubly fed induction generator using back–to–back PWM converters and its application to variable–speed wind–energy generation. *IEE Proc Electr Power Appl*. 1996;143(3):231–241.
11. Bauer J. Single Phase Voltage Source Inverter Photovoltaic Application. *Acta Polytechnica*. 2010;50(4):7–11.
12. Teodorescu R, Blaabjerg F. Flexible Control of Small Wind Turbines with Grid Failure Detection Operating in Stand–Alone and Grid–Connected Mode. *IEEE Trans Power Electron*. 2004;19(5):1323–1332.
13. Gan Dong. Sensorless and Efficiency Optimized Induction Machine Control with Associated Converter PWM Modulation Schemes, Tennessee Technological University, USA; 2005.
14. Perdana, Carlson O, Persson J. Dynamic Response of Grid–Connected Wind Turbine with Doubly Fed Induction Generator during Disturbances. Nordic Workshop on Power and Ind. El. (NORPIE 2004), Trondheim, Norway; 2004.
15. Engelhardt S, Genius A. Measurements of doubly fed induction generator with optimized fault ride through performance.
16. Hentabli K, Benbouzid MEH, Pinchon D. CGPC with Internal Model Structure: Application to Induction Motor Control. *In Proceeding of IEEE Control Appl*. 1997:235–237.
17. Peterson. Analysis, Modeling and Control of Doubly–Fed Induction Generators for Wind Turbines, Thesis for the degree of Doctor of Philosophy, Chalmers University of Technology, Sweden; 2005.
18. Harnefors L, Nee HP. Model–Based Current Control of AC Machines Using the Internal Model Control Method. *IEEE Trans Ind Applicat*. 1998;34(133):141.